Proceedings of the RAAD 2013
22nd International Workshop on Robotics in Alpe-Adria-Danube Region
September 11-13, 2013, Portorož, Slovenia

Inertial aided sensor platform stabilization for multirotor aerial vehicles

Igor Cvišić[a] and Ivan Petrović[a]

[a]*Department of Control and Computer Engineering,*
Faculty of Electrical Engineering and Computing,
University of Zagreb, Unska 3, 10000 Zagreb, Croatia
E-mail: {igor.cvisic,ivan.petrovic}@fer.hr

Abstract. Multiple rotor Unmanned Aerial Vehicles (UAVs) are becoming ubiquitous because of their construction simplicity and ease of maintenance. Such UAVs are able to hover, take off and land vertically. In addition, it is straightforward to design an on-board attitude autopilot. In comparison with classical helicopters, multi-rotor aircrafts provide less dangerous testbed in urban and cluttered environments due to their small-size and light-weight blades. In this paper, we present our prototype of aerial vehicle with eight rotors, which carries a unique platform for exteroceptive sensors. We designed inertial aided stabilization of the movement of the platform, decoupling the motion of exteroceptive sensors from the vehicle motion. This directly contributes to improved position and attitude estimation in visual navigation and smoother perception of the environment, and indirectly to achievement of the vehicle autonomy in urban and cluttered environments. The functionalities of the prototype aerial vehicle and the stabilizing platform are tested in simulation and experimentally.

Keywords. UAV, multirotor, sensor stabilization

1. Introduction

Multirotor aerial vehicles, with various construction designs, controllers and propulsion systems are taking their place amongst hobbyists, government services, industry applications etc. Furthermore, their popularity in the research community increased over the last couple of years. Many authors found these flying platforms interesting as test platforms for their algorithms, but unintentionally ignored the fact that these platforms could be very useful in many real life applications. Many teams have concentrated on complex algorithms which can perform fast and high-precision, but mostly not applicable acrobatics. We are motivated by the idea of enabling those machines to do useful real life tasks, making them safe, autonomous, reliable and competitive for various actions in open spaces and urban areas.

Motivated by this idea we have successfully designed and built an autonomous, small areal vehicle with redundant number of rotors, capable of lifting over 3 kg of payload. This aerial vehicle was used in many experiments, testing robustness to wind disturbance, tolerance to motor failure, autonomous flight using GPS etc. Outdoor environment is very unpredictable, and the wind is almost always present, especially at greater altitudes. Therefore, constant variation of vehicle's attitude, as a reaction to wind gusts, is inevitable. This can drastically deteriorate the signal quality from exteroceptive sensors. Images from the camera become blurred, GPS sensor reads Doppler velocities coupled from vehicle rotation, LIDAR scans are not lines any more etc. This behavior increases the uncertainty of estimated position of the aerial vehicle and distorts the map of surrounding. Some researches recover the original signal by compensating it with known vehicle rotation. If the sensor is a camera, image processing can be used (Wang et al., 2011). But when the obtained image is blurred, the needed information is unrecoverable.

Some researches presented their work related to camera teleoperation, visual servoing and target tracking. In these papers, image stabilization arose as a secondary problem. Mathematical models are often presented without considering the possibility of practical implementation. Equations of motion for a two-axis, pantilt, gimbal system to simplify the gimbal control were presented (Yoon and Lundberg, 2001). Problem of camera targeting was presented in (Chitrakaran et al., 2006) and (Neff et al., 2007) where a camera platform, a quadrotor UAV, and a camera positioning unit are considered to be controlled simultaneously. The work (Stolle and Rysdyk, 2003) proposed a solution to a problem of limited range of a camera mechanical positioner. Software-based camera control was presented by (Pieniazek, 2003),

and stabilization for two degree-of-freedom onboard camera to stabilize the image when the aircraft attitude was disturbed by turbulence or attitude changes.

In this paper we propose inertial aided stabilization of the platform with exteroceptive sensors, decoupling its motion from the motion of the vehicle. Sensor stabilization can advance visual navigation in outdoor environments, improve position and attitude estimation and clarify the perception of environment. High quality stabilization is obtained with low-cost and easily available parts, where further improvements are also possible.

Inertial aided stabilization corrects all types of distortions. Also, several sensors can be mounted on the same mechanically decoupled platform. It provides unique solution for solving different kinds of problems.

2. Standard approach to sensor platform stabilization

Doing experiments with an aerial vehicle in outdoor environments, we soon found out that without sensor platform stabilization it would be difficult to achieve autonomy of the vehicle navigation in outdoor environments. Our first approach, we named it here as standard approach, was pretty much straight-forward. We developed a sensor platform with two servo motors, which enabled platform tilting in all directions. By using the information about the roll and pitch angles from existing sensors on aerial vehicle, and by tilting the servo motors for the same amount in the opposite directions, the platform level could be stabilized. Fig. 1 shows the standard stabilized platform prototype. This approach will work well when dynamics of aerial vehicle is low and the movements are smooth. However, that is usually not the case in outdoor environments and this approach reveals two major weaknesses - inadequate speed of reaction and backlash. In order to have precise positioning and large torque, servo motors use gears with very high gear ratio. Output shaft has limited rotational speed and cannot follow the dynamics of the vehicle. Constant lag is present between the stabilized platform and the aerial vehicle. Second, the attitude of aerial vehicle continuously oscillates around the level position, forcing the servo gears to go back and forth and expose to the backlash. In applications where smooth signal is more important than absolute accuracy, backlash can be a bigger problem than speed of reaction itself. Beside nonlinearities and sudden jerks, consequences of the backlash existence are also vibrations in dead band area. Stabilizing platform can move freely in that band and can easily fall into resonance, especially in case of aerial vehicle motors vibration, attitude oscillation or/and direct wind. Although the dead band is usually measured in tenths of degree, it is large enough to cause blurred image or to affect laser measurement. Fig. 2 shows simulation results of the stabilizing platform angle θ for vehicle oscillations of angle α with amplitude 45 degrees and frequency 1 Hz. It can be seen that amplitude of the platform angle oscillations is about 6 degrees, which is too high.It is important to notice that amplitude of the oscillations for this stabilization approach would increase with frequency of vehicle oscillations due to inadequate reaction speed of the servo drives.

Fig. 1. Standard stabilization platform

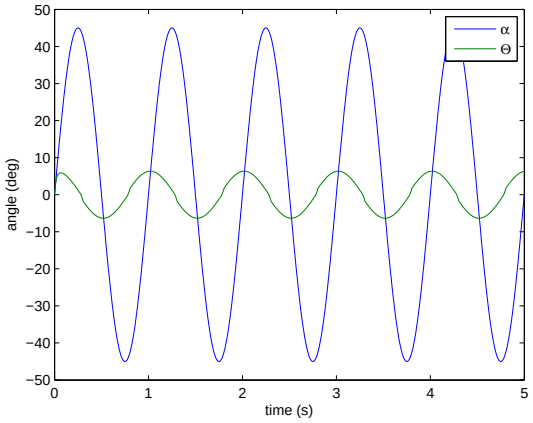

Fig. 2. Standard approach simulation

3. Inertial aided sensor stabilization platform

Analyzing the abovedescribed standard stabilizing platform with two servo motors, one can see that increasing the servo speed cannot completely solve the problem. The problem lays in a fact that, in order to compensate for the aerial vehicle movement, the information is needed that the vehicle movement has happened. At the moment when this information is received by the platform servo control system it is

already too late, as the platform has already moved at least a little bit together with the vehicle.

In order to avoid direct influence of aerial vehicle rotation to the stabilized platform rotation, one can put the stabilized platform on a gimbal in such a way that the platform rotates freely in a ball bearings (Fig. 3). In ideal case, if one adjusts platforms center of gravity (CG) with the gimbal axis, linear and rotational movement of the vehicle will not disturb the attitude of the platform. In addition, one can increase the moment of inertia of the platform to create higher resistance to external forces, such as the wind and tension from sensor cables, and produce a smoother motion. Rotational inertia of the platform can be increased by separating the platform into two parts of similar weights, mounted on the opposite ends of a pole. Aerial vehicle's battery can be used as a counterweight to the sensors, and the CG can be adjusted with the position of the battery. In this way rotational inertia is increased significantly, while the total weight is increased only by the mass of the pole. Carbon fiber tube, which is very lightweight, can be used as a pole. Now the rotational dynamics of the platform is low and external forces can not cause sudden change in its attitude. However, those external forces will act on the platform continuously during the flight, and gradually, platform will drift from desired position. Furthermore, in reality, one can not perfectly align CG with axis of rotation, and acceleration forces will also cause undesirable rotational movement of the platform.

Due to the circumstances described above, some kind of control mechanism for the platform must be implemented. If we install any hard linkage between aerial vehicle and the sensor platform in order to control the platform, vehicle rotation will be directly transferred to the platform. Therefore, in order to benefit from high moment of inertia of the platform, we propose a soft linkage between the aerial vehicle and the sensor platform. One way to do this is usage of the electro-magnetic field, e.g. with a DC motor aligned with the axis of rotation. If the motor is disconnected it behaves just like a ball bearing, and the platform can rotate freely. By controlling the motor current, one can control the torque and compensate for external forces when necessary. However, in that case motor can not use gear reduction to produce needed torque, because gears make hard linkage to the aerial vehicle. Motors that create large enough torque directly on their output shaft are often too large and heavy for aerial vehicle. Also, motors suffer from cogging, an interaction between permanent magnets on the rotor and slots on the stator. When disconnected, the motor does not move freely like the ball bearing. Instead, cogging torque causes jerkiness, which is especially prominent at low speeds, such as in this application.

Drawbacks of using gearless motor as soft linkage between the vehicle and the platform, motivate our solution, which is moreover much simpler. We use springs as the linkage between stabilizing sensor platform and the vehicle (Fig. 3). One can control the attitude of the platform by controlling the tension of the springs. Unlike motors with cogging, springs have very smooth force curve and cheap servo motors can be used to control their tension. However, springs do not completely decouple platform rotation from the vehicle rotation, like disconnected motor in the first case. Springs alone just provide a delayed rotation of the platform caused by the vehicle rotation. One can use that delay as an elegant solution to a problem of limited reaction speed of the servo drives. Upon sudden change in vehicle's attitude, at the first moment while control system is not able to react, springs will absorb the energy and high moment of inertia will hold the platform still. Method with springs introduces delay into the process, which is greater than delay in the control system. This makes control system very fast relative to process and solves the problem of inadequate speed of reaction.

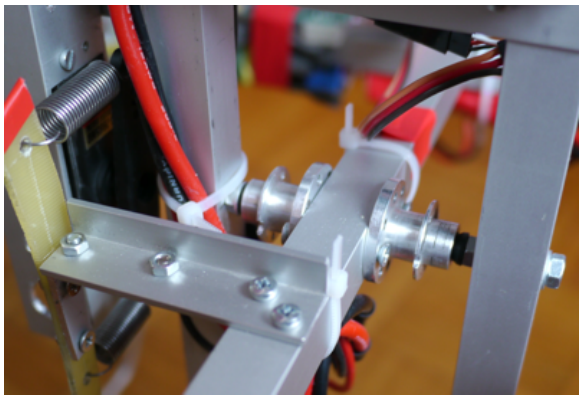

Fig. 3. Ball bearings with springs on prototype vehicle

4. Control of the proposed stabilizing platform

4.1. Mathematical model

Fig. 4 shows the principle of stabilization method in one dimension.

The aerial vehicle and the platform are mechanically connected through a common axis of rotation with the ball bearings. Platform has a servo motor with the servo arm that can rotate around the same axis of rotation as the platform. Angle β between the servo arm and the platform is the angle that we can control. Tilt of the platform is represented by the angle θ, and we want to keep that angle as close as to zero. During the flight, the vehicle angle α changes through the time with a rate proportional to vehicle dynamics. We can represent the whole system with the input angle β, output angle θ and disturbance α.

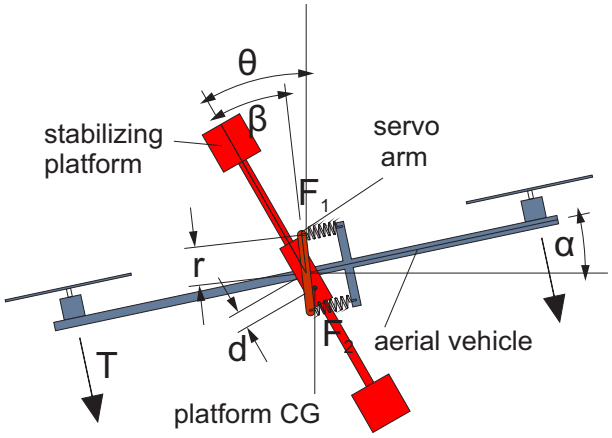

Fig. 4. Stabilization platform with springs - principle scheme

Servo arm is connected to the aerial vehicle by two tensional springs with tension forces F_1 and F_2. Given that $\beta = -(\theta - \alpha)$, springs are equal in length, $F_1 = F_2$ and resulting torque is zero.

Summing the forces on the vehicle in horizontal direction gives the

$$\begin{aligned}(M+m)\ddot{x} + B\dot{x} = \\ -md\ddot{\theta}cos(\theta) - Tsin(\alpha) + d\dot{\theta}^2 sin(\theta),\end{aligned} \tag{1}$$

and summing the moments on the stabilized platform gives

$$\begin{aligned}(I+md^2)\ddot{\theta} + mgdsin(\theta) + md\ddot{x}cos(\theta) + b\dot{\theta} = \\ -2r^2 ksin(\theta+\beta-\alpha)\end{aligned} \tag{2}$$

where:

- M - mass of the vehicle $[kg]$,
- B - air resistance of the vehicle $[\frac{Ns}{m}]$,
- m - mass of the stabilized platform $[kg]$,
- m - air resistance of the platform $[\frac{Ns}{m}]$,
- I - moment of inertia of the platform $[kgm^2]$,
- k - spring constant $[\frac{N}{m}]$,
- r - half-length of the servo arm $[m]$,
- x - horizontal position of the vehicle $[m]$,
- T - thrust force $[N]$
- d - distance from platforms CG to the rotational axis $[m]$.

The system model (1) and (2) is nonlinear but we can linearize it. First, the angle of the stabilized platform θ will be zero in equilibrium position, during stabilization it will always follow the zero reference and we can assume that it will be very close to zero. Therefore, we can write following approximations:

$$\begin{aligned}cos(\theta) &\approx 1 \\ sin(\theta) &\approx \theta \\ \dot{\theta}^2 &\approx 0.\end{aligned} \tag{3}$$

Second, since the vehicle equilibrium is hover position, $\alpha = 0$, vehicle will mostly operate around hover position and in practice α will rarely go beyond 30 degrees, the following approximation can be applied:

$$sin(\alpha) \approx \alpha. \tag{4}$$

Also, for simplicity, we can consider a constant thrust. In practice, multirotor is mostly operating in horizontal plane of a fixed altitude, and the thrust is varying around the $T = (M+m)g$. Finally, given the previous description of the system itself, we know that the platform tends to stay still, and the system needs to apply only small corrections against disturbance and disbalance, with average torque of zero. We can linearize the right side term of equation (2) around the zero torque $\beta \approx -(\theta - \alpha)$ and make an additional simplification

$$sin(\theta+\beta-\alpha) \approx \theta+\beta-\alpha. \tag{5}$$

By applying the above approximations we get the model linearized around the operating point

$$(M+m)\ddot{x} + B\dot{x} + md\ddot{\theta} + T\alpha = 0, \tag{6}$$

$$(I+md^2)\ddot{\theta} + mgd\theta + md\ddot{x} + b\dot{\theta} + 2r^2 k(\theta+\beta-\alpha) = 0. \tag{7}$$

Taking the Laplace transform and solving this system of equations by eliminating x we get the transfer function of the system

$$\Theta(s) = G_\alpha(s)\alpha(s) - G_\beta(s)\beta(s), \tag{8}$$

where

$$G_\beta(s) = \frac{\frac{M_m Rk}{q}s + \frac{BRk}{q}}{s^3 + \frac{M_m b + B(I+md^2)}{q}s^2 + \frac{M_m(mdg+Rk)+Bb}{q}s + \frac{mdgB+BRk}{q}}, \tag{9}$$

$$G_\alpha(s) = \frac{\frac{(M_m Rk+Tmd)}{q}s + \frac{BRk}{q}}{s^3 + \frac{M_m b + B(I+md^2)}{q}s^2 + \frac{M_m(mdg+Rk)+Bb}{q}s + \frac{mdgB+BRk}{q}}, \tag{10}$$

$$q = (I+md^2)M_m + m^2 d^2, \tag{11}$$

$$R = 2r^2 \tag{12}$$

and M_m is the total mass

$$M_m = M + m. \tag{13}$$

Also, to have a complete model of the system, we must model the transfer function of the servo used. Neglecting the electrical subsystem component of the DC motor model and representing it only with dominant mechanical subsystem one can write the simplified transfer function of the DC motor

$$DC(s) = \frac{K}{\tau s + 1} \tag{14}$$

where K and τ are the dc-gain and the mechanical time-constant of the DC motor, respectively. Servo is controlling DC motor velocity in its outer position loop with PD controller. Substituting motor equation above into PD controller gives transfer function of the servo

$$A(s) = \frac{KK_p}{\tau s^2 + (1 + KK_D)s + KK_P} \tag{15}$$

where K_P and K_D are the proportional and derivative component of the PD controller, respectively.

4.2. Feedback control loop

Block diagram of the feedback control of the platform angle θ is depicted in Fig. 5. For controlling the angle θ we have used a controller $K(s)$ of the PID type, which parameters are tuned by the autotuning procedure given in (Peric et al., 1997).

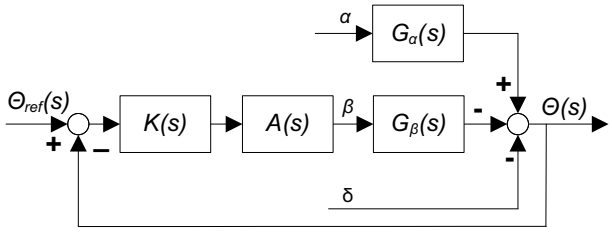

Fig. 5. Block diagram of the control system

Fig. 6 shows the angle of the stabilized platform in response to disturbance α - aerial vehicle angle. Disturbance is set as a sine with amplitude of 45 deg and period of 1 rad/sec. We can see that softest springs give the best results. However, decreasing the k also decreases the maximal torque we can produce. Relative airflow will produce a drag force on the sensor (Hull, 2007),

$$F_d = \frac{1}{2}\rho v^2 C_d A, \tag{16}$$

where ρ is the density of the fluid, v is the speed of the object relative to the fluid, A is the cross-sectional area, and C_d is the drag coefficient. Just to be in the right order of magnitude, we have calculated the drag force for a ball of a radius of 10 cm with a relative airspeed of $3m/s$. We have simulated a short wind impact with resulting drag force applied to the sensor. Results of a simulation test are shown in Fig. 7. For $k = 10$ and below system cannot give enough torque to oppose external forces. Graph also shows that for k too large system becomes unstable. That is because PID parameters were constant for all k to emphasize dependence on k. PID tuning should be done after every change of k.

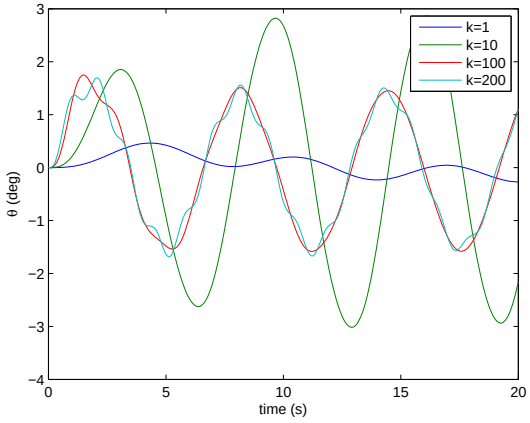

Fig. 6. Response to change in vehicles attitude with constant d

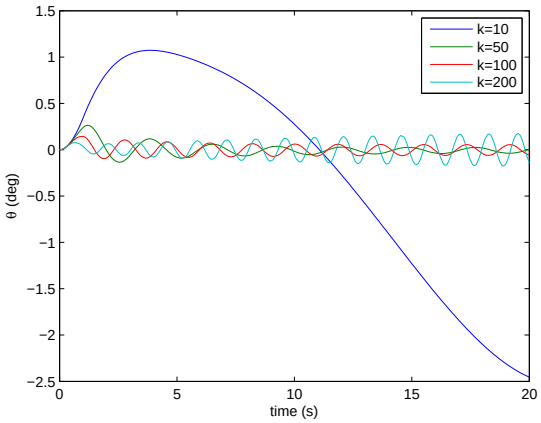

Fig. 7. Response to external disturbance

4.3. Perfect balance

Setting the perfect balance for the platform would decouple rotation of the platform from vehicle acceleration. Substituting $d = 0$ into our equations (9),(10) and (11) yields

$$q = M_m I, \tag{17}$$

$$G_\alpha(s) = \frac{M_m Rks + BRk}{M_m Is^3 + (M_m b + IB)s^2 + (M_m Rk + Bb)s + BRk}, \tag{18}$$

Rearranging, we get

$$G_\alpha(s) = \frac{Rk(M_m s + B)}{Is^2(M_m s + B) + bs(M_m s + B) + Rk(M_m s + B)}, \tag{19}$$

and finally

$$G_\alpha(s) = \frac{Rk}{Is^2 + bs + Rk}. \tag{20}$$

Equivalently,

$$G_\beta(s) = G_\alpha(s) = \frac{Rk}{Is^2 + bs + Rk}. \tag{21}$$

4.4. Optimal point for center of gravity

Fig. 8 show dependence of stabilization with respect to various positions for CG. We can see that perfect balance does not have a minimal error. To obtain the minimal influence of α on θ one must set the nominator of G_α to zero (Equation (10)). Since $M_m Rk >> BRk$, neglecting the smaller term gives

$$M_m Rk + Tmd = 0 \tag{22}$$

In practice, adjusting the CG to

$$d = -\frac{2(M+m)r^2 k}{Tm} \tag{23}$$

decreases sensitivity to the change of α. Negative d means that CG should be slightly above the axis of rotation, creating a kind of inverted pendulum. Physically, what happens is that positive angle α creates a positive torque on the platform through the tension of the springs, but at the same time it projects the thrust in horizontal plane that will accelerate the vehicle, and that acceleration force will create negative torque of the same amount on the platform if d is set according to Equation (23). In practice, such precise balancing is hard to perform and we cannot expect to have d exactly as we want to. Also, this equation came from linearized model and completely canceling the influence of α just with selection of d is not possible neither mathematically.

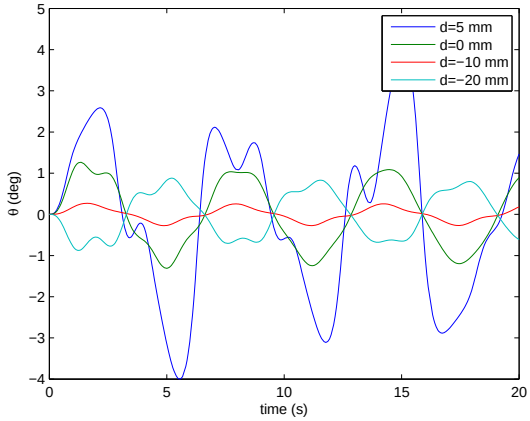

Fig. 8. Response to change in vehicles attitude with constant k

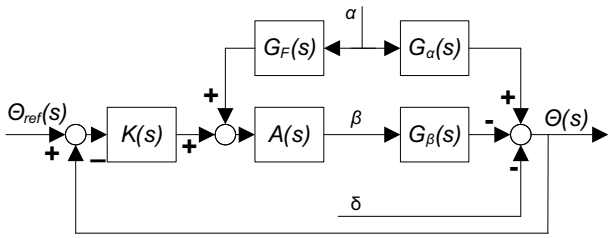

Fig. 9. Block diagram of the control system with the feedforward loop

4.5. Feedforward control loop

Since external disturbance δ cannot be predicted, only improvement we could think of regarding δ would be an aerodynamical case for sensor placement. However, aerial vehicle attitude angle α is known and its influence on θ is predictive. Introducing a feedforward transfer function G_F one can represent this new system with Fig. 9 To cancel out disturbance α following equation must be satisfied

$$G_\alpha(s) = G_F(s)A(s)G_\beta(s) \tag{24}$$

Solving for G_F yields

$$G_F(s) = \frac{(M_m Rk + Tmd)s + BRk}{(M_m Rk)s + BRk}\frac{1}{A(s)} \tag{25}$$

Looking at equation for $A(s)$, we can see that it multiplies numerator to have higher order terms than denominator, making this transfer function impossible to realize. We will have to simplify $A(s)$ to its constant gain in order to realize G_F in practice

$$A(s) \approx 1 \tag{26}$$

to have

$$G_F(s) = \frac{(M_m Rk + Tmd)s + BRk}{(M_m Rk)s + BRk} \tag{27}$$

Fig. 10 shows simulated response of the system. Note the improvement over the Fig 6. For every selection of k an error is bounded below 0.1 degrees. For a better comparison, PID parameters are not changed with introduction of feedforward. In practice, implementing a feedforward function requires a knowledge of d. Easiest way for implementing feedforward is setting the platform close to the perfect balance as possible, for a feedforward function to become

$$G_F(s) = 1. \tag{28}$$

5. Experimental results

We have made an experimental platform (see Fig. 11) for presented system. Attitude of stabilized platform is measured with $MPU6050$ sensor, and the flight controller is from our previous work (Cvisic and Petrovic,

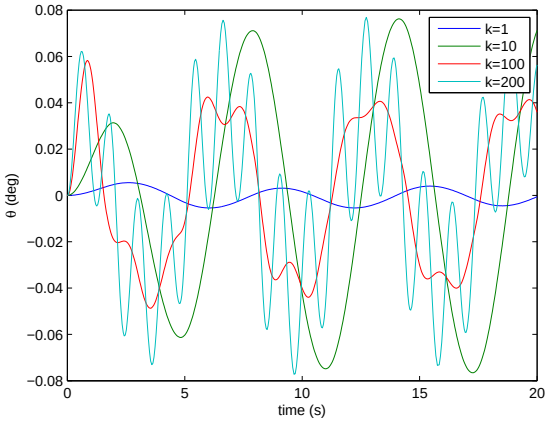

Fig. 10. Feed forward response to change in vehicles attitude

Fig. 11. Experimental aerial vehicle in flight

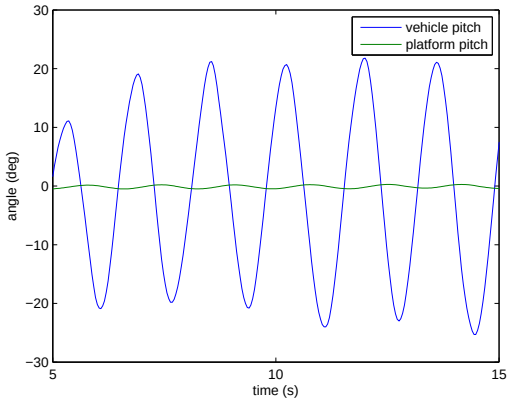

Fig. 12. Platform angle recorded from experiment

2013). Stabilizing platform controller is tuned with relay feedback method (Peric et al., 1997). We have used balanced platform and feedforward with gain of 1. Fig. 12 shows platform angle recorded during the high frequency disturbance α. We have recorded a platform oscillation with amplitude of approx. 0.3 degrees caused by a vehicle oscillation with amplitude around 20 degrees. Fig. 13 shows 10 seconds long part of the flight. Platform angle is bounded to half of degree. Results from experiments are satisfactory, although simulation gave slightly better results. We suspect that the main reason for discrepancies from simulation are caused by tension from power cables and disbalance. Vehicle battery is used as a counterweight, and the power cables from battery must carry out from stabilized platform through the vehicle to the propulsion motors. Although we have used soft silicone cables arranged to give minimum resistance to movement of the platform, cables must be thick enough to carry at least 50 amperes of current and small tension between vehicle and platform is inevitable. Putting the battery directly on the vehicle and using a dummy weight as a counterweight is not acceptable, because it brings unnecessary weight to the vehicle, overloads the system, shortens the flight time and disables the practical use of the vehicle.

6. Conclusion

We have addressed the problem of mounting exteroceptive sensors on the multirotor aerial vehicles. We have analyzed various possible solutions and decided for an inertial method with springs. We have set the model of the system and tested it in a simulator. Then we have built a prototype of a stabilization platform, modified the construction of the experimental aerial vehicle to handle the platform and tested the system in a real outdoor flight. Experimental results showed slightly greater deviation than expected according to simulator. We explain that by windy conditions, tension of the power cables and not perfect balance. We would expect much better results if a prototype would be built with a more precise, industrial grade parts. Also, enclosing the upper and lower weight in an aerodynamic case would reduce the sensitivity to wind. It is convenient to have a modular system that can enable the user to mount various types of sensors. That way, the user should re-balance the system by itself and one cannot expect perfect factory balance. For our future work, we consider an online estimator of the CG from measured angles and accelerations. Then we could use feedforward function to cancel out disbalance of the platform.

7. Acknowledgments

This work has been supported by the European Communitys Seventh Framework Programme under grant agreement no. 285939 (ACROSS).

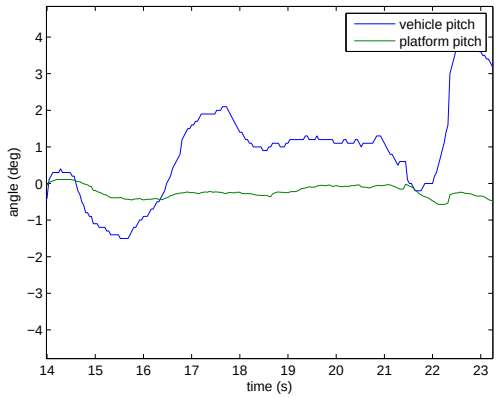

Fig. 13. Platform angle during the flight

8. References

Chitrakaran, V., Dawson, D. M., and Kannan, H. (2006). Vision assisted autonomous path following for unmanned aerial vehicles. In *in Proc of 45th IEEE Conference on Decision and Control, pp. 63 - 68, Dec. 2006.*

Cvisic, I. and Petrovic, I. (2013). Development and testing of small aerial vehicles with redundant number of rotors.

Hull, D. (2007). *Fundamentals of Airplane Flight Mechanics*. Springer.

Neff, A., Lee, D., Chitrakaran, V., Dawson, D. M., and Burg, T. C. (2007). Velocity control of a quadrotor uav fly-by-camera interface. In *in Proceedings of IEEE Southeast Conference, pp. 273-278, Richmond, VA, Mar. 2007.*

Peric, N., Petrovic, I., and Branica, I. (1997). A method of pid controller autotuning. In *Commande des systemes industrieles - Control of Industrial Systems, Belfort, France, May 20-22, 1997, pp. 43–48.*

Pieniazek, J. (2003). Software-based camera stabilization on unmanned aircraft. In *Aircraft Engineering and Aerospace Technology: An International Journal, Vol. 75, No. 6, 2003, pp. 575 580.*

Stolle, S. and Rysdyk, R. (2003). Flight path following guidance for unmanned air vehicles with pan-tilt camera for target observation. In *in Proceedings of the AIAA Digital Avionics Systems Conference, Oct. 2003, pp 01 12.*

Wang, Y., Hou, Z., Leman, K., and Chang, R. (2011). Real-time video stabilization for unmanned aerial vehicles.

Yoon, S. and Lundberg, J. B. (2001). Equations of motion for a two-axes gimbal system. In *IEEE Transactions on Aerospace and Electronic Systems, Vol. 37, No. 3, July 2001, pp. 1083 1091.*